

# Dynamic compression of SiO<sub>2</sub>: A new interpretation

Joseph A. Akins and Thomas J. Ahrens

Lindhurst Laboratory of Experimental Geophysics, Seismological Laboratory 252-21, California Institute of Technology, Pasadena, CA, USA

Received 25 January 2002; revised 1 April 2002; accepted 3 April 2002; published 22 May 2002.

[1] In light of recent discoveries of post-stishovite phases of SiO<sub>2</sub>, with the CaCl<sub>2</sub> and  $\alpha$ -PbO<sub>2</sub> structures, we have reassigned the regimes along the Hugoniot for initial quartz, coesite, cristobalite, porous coesite, and fused silica. Calculated Hugoniot for fused silica, cristobalite and porous coesite indicate transition to stishovite, and then melt. Hugoniot for crystal quartz and coesite indicate that transition occurs to stishovite, then the CaCl<sub>2</sub> structure and finally to melt. **INDEX TERMS:** 8147 Evolution of the Earth: Planetary interiors (5430, 5724); 3919 Mineral Physics: Equations of state; 3944 Mineral Physics: Shock wave experiments; 3924 Mineral Physics: High-pressure behavior; 5460 Planetology: Solid Surface Planets: Physical properties of materials

## 1. Introduction

[2] The recent discoveries that pure silica transforms to the CaCl<sub>2</sub> ( $\rho_0 = 4.291 \text{ g/cm}^3$ ) and  $\alpha$ -PbO<sub>2</sub> ( $\rho_0 = 4.334 \text{ g/cm}^3$ ) structures, slightly more dense than stishovite ( $\rho_0 = 4.287 \text{ g/cm}^3$ ), have led to a reexamination of the dynamic compression of SiO<sub>2</sub>. Although the first observation of the CaCl<sub>2</sub> structure indicated it was stable above  $\sim 100 \text{ GPa}$  [Tsushida and Yagi, 1989] later theoretical [Cohen, 1991] and experimental [Andrault et al., 1998; Dubrovinsky et al., 1997; Kingma et al., 1995] studies have constrained the onset of the stishovite to CaCl<sub>2</sub> transition to  $\sim 50 \text{ GPa}$  at 298 K. The  $\alpha$ -PbO<sub>2</sub> structure is found to be stable above  $\sim 80 \text{ GPa}$ , based on experiments and theoretical calculations [Dubrovinskaia et al., 2001; Dubrovinsky et al., 2001; Dubrovinsky et al., 1997, 2001; Teter et al., 1998]. The  $\alpha$ -PbO<sub>2</sub> structure has also been observed in the Shergotty meteorite, a Martian basalt thought to have experienced multiple shock events [El Goresy et al., 2000].

[3] In addition to these high-pressure silica phases, with oxygen in 6-fold coordination, transition to an 8-fold coordination structure is predicted near 200 GPa [Dubrovinsky et al., 1997; Teter et al., 1998]. Although it is unclear whether substantial quantities of a phase of SiO<sub>2</sub> exists in the Earth's mantle, the equation of state of the high-pressure SiO<sub>2</sub> phases play a crucial role in mantle-core chemical reactions which sequester iron from mantle silicates into the core [Luo et al., 2002].

[4] Crystal and fused silica were the first silicates studied by dynamic compression methods [Adadurov et al., 1962; Wackerle, 1962]. Thereafter McQueen et al. [1963] demonstrated that the Hugoniot of crystal ( $\rho_0 = 2.65 \text{ g/cm}^3$ ) and fused silica ( $\rho_0 = 2.2 \text{ g/cm}^3$ ), above 40 GPa, correspond to the properties of the rutile structure of SiO<sub>2</sub> [Stishov and Popova, 1961], which was later found in shocked quartz-bearing rocks of Meteor Crater [Chao et al., 1962]. Subsequently, small amounts of stishovite were recovered from peak pressures in the 15–28 GPa range [DeCarli and Milton, 1965].

[5] Additional studies of quartz and fused silica, as well as cristobalite ( $\rho_0 = 2.13 \text{ g/cm}^3$ ), porous coesite ( $\rho_0 = 2.4 \text{ g/cm}^3$ ), coesite ( $\rho_0 = 2.92 \text{ g/cm}^3$ ), and stishovite ( $\rho_0 = 4.31 \text{ g/cm}^3$ ) have been conducted by Fowles [1967], Trunin et al. [1971], Podurets et al. [1990], Borshchevskii et al. [1998], Lyzenga et al. [1983], Zhugin

et al. [1999] and Luo et al. [2002]. With the exception of the more scattered fused silica results, we take these data together and point out that strong evidence exists for the transitions to stishovite, the CaCl<sub>2</sub> structure and melt along the Hugoniot of quartz and coesite, whereas, cristobalite and porous coesite melt directly from the stishovite regime.

## 2. Dynamic Compression of Crystal Quartz

[6] The outline of our interpretation of the crystal quartz Hugoniot is shown in Figure 1. Theoretical calculations for Hugoniot pressure-density and pressure-temperature for crystal quartz (and other SiO<sub>2</sub> phases) of Figures 1–4 are based on the Mie-Grüneisen offset from the 3rd order Birch-Murnaghan isentropes (e.g. McQueen et al. [1963]). We infer from the phase diagram of Figure 4 and the independent pressure-density and pressure-temperature Hugoniot data for various silica phases, there are the following eight regimes along this Hugoniot: 1) The elastic shock Hugoniot extending to 5.5–15.0 GPa depending on orientation [Fowles, 1967; Wackerle, 1962]. 2) The quartz deformational Hugoniot extending from 15 to 23 GPa [Zhugin et al., 1999]. 3) Mixed phase regime (A) of quartz and stishovite extending from 23 to 35 GPa [Zhugin et al., 1999]. 4) The stishovite regime from 35 to 70 GPa, which is consistent with the equation of state (EOS) parameters for stishovite in Tables 1 and 2. 5) Mixed phase regime (B) of stishovite and CaCl<sub>2</sub> ( $\sim 70 \text{ GPa}$ ). 6) The CaCl<sub>2</sub> structure regime from 70 to 115 GPa. The Hugoniot in this regime is consistent with parameters for CaCl<sub>2</sub> structure given in Tables 1 and 2. 7) Mixed phase regime (C) of CaCl<sub>2</sub> and melt. 8) The melt regime  $>120 \text{ GPa}$ . Previous analyses of these data fit regions 4–7 together as a single phase. The Hugoniot from 120–200 GPa is consistent with the melt EOS parameters in Tables 1 and 2 and is assumed to be in 6-fold coordination. We propose that a transition to 8-fold coordination begins at  $\sim 200 \text{ GPa}$ .

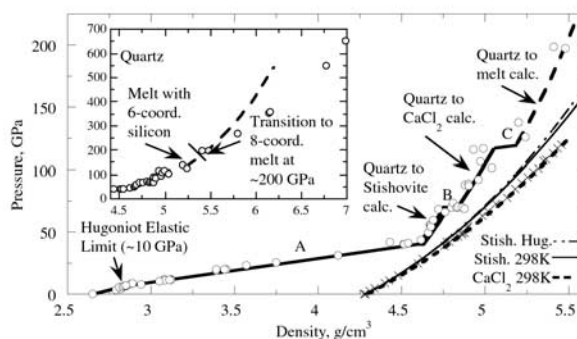


**Figure 1.** New interpretation of Hugoniot of crystal SiO<sub>2</sub> (quartz). Data (circles) from Marsh [1980], Fowles [1967], Trunin et al. [1971], Lyzenga et al. [1983], Podurets et al. [1976, 1990], Borshchevskii et al. [1998]. Static compression data for initially stishovite (x's) from Andrault et al. [1998]. Curves in stishovite, CaCl<sub>2</sub> and melt regime calculated from parameters of Table 1.

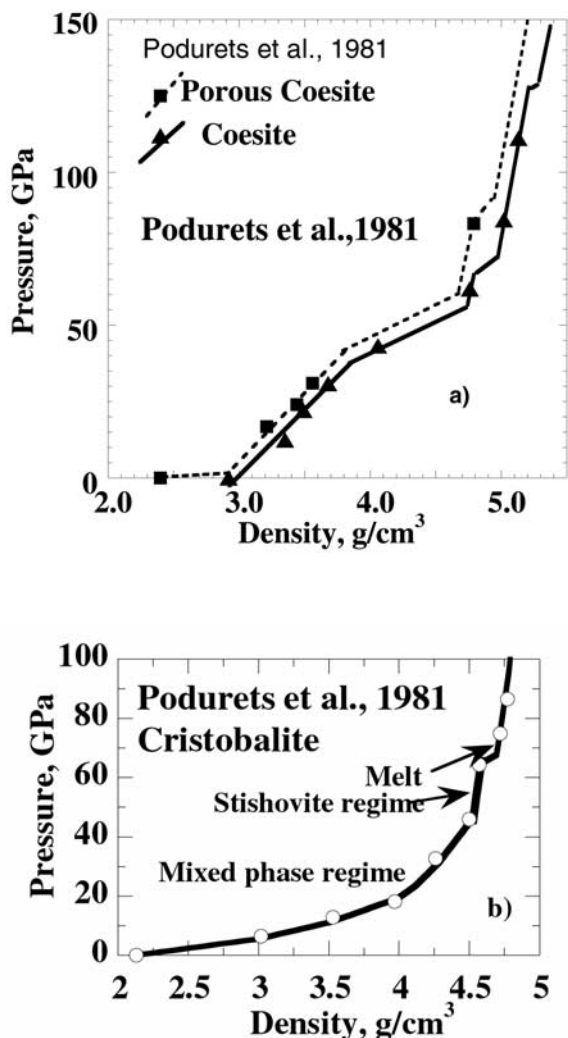


**Figure 2.** (a) Hugoniot data, initially porous ( $\rho_0 = 2.4 \text{ g/cm}^3$ ) and polycrystalline ( $\rho_0 = 2.92 \text{ g/cm}^3$ ) coesite. (b) Hugoniot data, cristobalite ( $\rho_0 = 2.13 \text{ g/cm}^3$ ).

[7] The compression of stishovite and the  $\text{CaCl}_2$  structure, observed in the diamond anvil study of *Andraut et al.* [1998] (and references therein) are plotted below the shock wave data in Figure 1. Notably the diamond anvil data displays a transition at  $\sim 54 \text{ GPa}$  from stishovite to the  $\text{CaCl}_2$  structure in approximate agreement with the deviation of the calculated 298K isotherms of stishovite and the  $\text{CaCl}_2$  structure.

### 3. Coesite, Porous Coesite, and Cristobalite Data

[8] Shock data for coesite ( $\rho_0 = 2.92 \text{ g/cm}^3$ ) and porous coesite ( $\rho_0 = 2.4 \text{ g/cm}^3$ ) are plotted in Figure 2a. The theoretical Hugoniot curves are consistent with the stishovite,  $\text{CaCl}_2$  and melt EOS parameters of Tables 1 and 2. Coesite and porous coesite are assessed to transform to stishovite above 30 GPa. The single datum for porous coesite at 85 GPa is assumed to correspond to a point in the stishovite-melt regime which achieves a higher density than stishovite. In contrast the single-crystal coesite achieves a state at 62 GPa, consistent with coesite transformed to stishovite, whereas the two-higher pressure states at 85 and 111 GPa appear to lie along the  $\text{CaCl}_2$  regime of the coesite Hugoniot; melt is inferred above 137 GPa. The coesite data of *Luo et al.* [2002] is consistent with this interpretation.

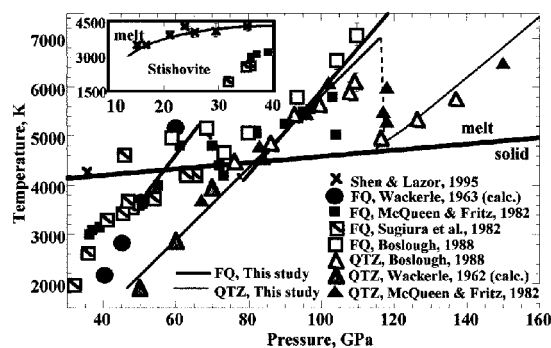


**Figure 3.** Hugoniot temperatures, fused quartz (FQ) and quartz (QTZ), *Lyzenga et al.* [1983] (with minor corrections for Al absorption, *Boslough* [1988]). Melting curve is shown for comparison.

[9] In the case of cristobalite data, Figure 2b, we interpret the point at 46 GPa as still being in the cristobalite-stishovite mixed-phase regime, the datum at 64 GPa as in the stishovite regime and the data at 75 and 86 GPa as in the dense  $\text{SiO}_2$  melt regime.

### 4. Shock Temperatures

[10] Complete shock temperature data for both fused silica and crystal quartz, as well as calculations in the solid and melt phases, are shown in Figure 3 and for the solid only in Figure 4 relative to our newly inferred high-pressure phase diagram of  $\text{SiO}_2$ . Shock temperatures were calculated using the method of *Ahrens et al.* [1982]. The calculated shock temperatures of *Wackerle* [1962] for both fused silica and crystal quartz are in remarkable agreement with *Lyzenga et al.* [1983] and *McQueen and Fritz* [1982] data. The fused silica shock temperatures below 55 GPa are in the stishovite stability field, the data between 55 and 65 GPa correspond to superheated stishovite, and above 75 GPa lie along the melt region of the Hugoniot. For crystal quartz the Hugoniot between 70 and 115 GPa is in the  $\text{CaCl}_2$  structure rather than

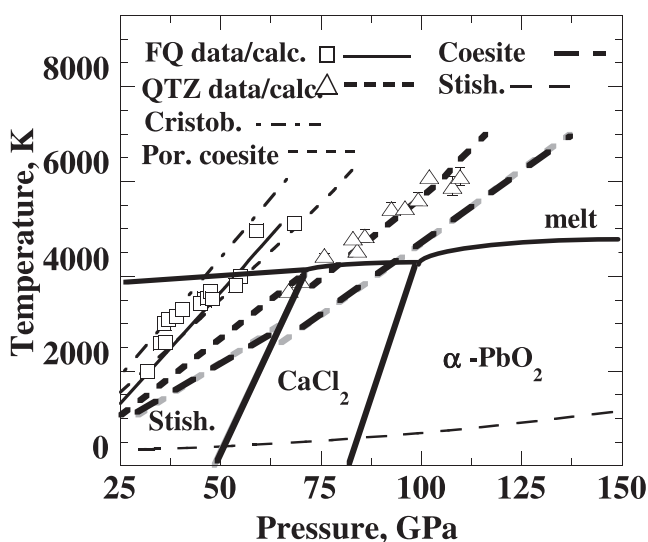


**Figure 4.** Proposed phase diagram of  $\text{SiO}_2$ . Only data and calculations for solid phases are shown. Shock temperature calculations are terminated at pressures corresponding to observed, or expected, drops in temperature due to melting. The field of  $\alpha\text{-PbO}_2$  is indicated for reference only.

**Table 1.** Thermodynamics Parameters

Phase	Initial Density, $\rho_0$ (g/cm <sup>3</sup> )	Bulk Modulus, $K_0$ (GPa)	$dK_0/dP$ , $K'$	Gruneisen Parameter, $\gamma_0$	$q^f$	Specific Heat, $C_v$ (J/kg K)
Stishovite	4.287 <sup>a</sup>	315 <sup>b</sup>	4.8 <sup>b</sup>	1.35 <sup>c</sup>	2.6	0.9 <sup>f</sup> 3nR <sup>c</sup>
CaCl <sub>2</sub>	4.291	291 <sup>d</sup>	4.3 <sup>d</sup>	1.4	1	0.9 <sup>f</sup> 3nR
melt	4.000	140	6.0	1.4	0.7	1.2 <sup>f</sup> 3nR

<sup>a</sup>Weidner *et al.* [1982].<sup>b</sup>Panero *et al.* [2000].<sup>c</sup>Stixrude and Bukowinski [1993].<sup>d</sup>Andraut *et al.* [1998].<sup>e</sup>n = 3 = # of atoms per formula unit.<sup>f</sup> $\gamma = \gamma_0(V/V_0)$ <sup>a</sup> Luo *et al.* [2002].

the superheated stishovite phase. Shock temperature states above 115 GPa are completely melted. The interpretation of super-heated solid followed by a drop in temperature due to melting is also supported by the post-shock temperature analysis of *Boslough* [1988]. Therefore the drop in shock temperature at 70–75 GPa for fused silica corresponds to catastrophic homogeneous melting [Lu and Li, 1998] of stishovite, whereas the drop between 115 and 120 GPa for shocked crystal quartz results from catastrophic homogeneous melting of crystal quartz transformed to the CaCl<sub>2</sub> structure.

[11] The shock temperature calculations (Figure 4) for cristobalite indicate that it enters the regime of transition to stishovite above 20 GPa and the molten SiO<sub>2</sub> stability field at 65 GPa. The pressure-density Hugoniot data clearly demonstrates that like fused silica transformed to stishovite, cristobalite also is superheated along the stishovite branch of its Hugoniot to shock pressures of 65 GPa (see Figure 2b) at which point it enters a stishovite-melt mixed-phase regime. The pressure-density data suggest that at ~70 GPa complete melting has occurred. Therefore we predict future shock temperature experiments will see a drastic decline in shock temperature from ~6000 to ~4000 K at ~70 GPa in cristobalite.

[12] Similarly, porous coesite appears to begin to transform to the stishovite structure above 30 GPa and is completely transformed into the stishovite regime at 55 GPa. Between 55 and 80 GPa it appears to remain in the stishovite structure although above 55 GPa the stishovite is superheated. The pressure-density data (Figure 2a) suggest that melting of the superheated stishovite occurs at ~85 GPa and above ~90 GPa the Hugoniot is inferred to be in the complete melt regime.

[13] We note that coesite also demonstrates the phase transition to stishovite starting at 30 GPa, and is driven into the coesite-stishovite mixed phase regime from 30 to 50 GPa and in the pure stishovite region from 50 to ~62 GPa. Transition from stishovite to the CaCl<sub>2</sub> structure appears to occur at ~65 GPa and superheating occurs up to ~7000 K. We infer that at ~137 GPa transition to the melt occurs. Coesite shocked into the CaCl<sub>2</sub> structure is superheated and extends metastably into the melt from ~80 to ~137 GPa. Given this new interpretation of the transformation from stishovite to the CaCl<sub>2</sub> structure along the quartz and coesite Hugoniots, at ~70 and ~65 GPa, respectively, the Clapeyron

slope of the transition is constrained to be ~180 K/GPa compared to 250 K/GPa predicted by *Kingma et al.* [1995].

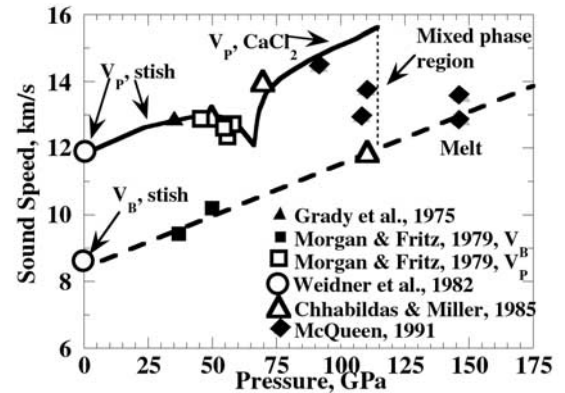
[14] Stishovite is too cold to undergo any of the above mentioned solid-solid phase transitions along its Hugoniot [Luo *et al.*, 2002]. We predict that stishovite will melt at ~425 GPa along its principal Hugoniot. To observe the solid-solid transitions, future shock experiments on porous stishovite, stishovite/coesite, or stishovite/paraffin mixtures are needed. For  $\rho_0 = 3.6$  g/cm<sup>3</sup> we predict the CaCl<sub>2</sub> to  $\alpha$ -PbO<sub>2</sub> transition will be observed at ~100 GPa and ~3000 K, and melting at ~200 GPa and ~6300 K. For  $\rho_0 = 3.95$  g/cm<sup>3</sup> we predict CaCl<sub>2</sub> to  $\alpha$ -PbO<sub>2</sub> at ~100 GPa and ~1600 K,  $\alpha$ -PbO<sub>2</sub> to 8-fold coordination solid at ~200 GPa and ~3500 K and melting at ~315 GPa and ~6500 K.

## 5. Hugoniot Sound Velocities

[15] The measurements of sound velocity behind the shock front in dynamically compressed crystal quartz ( $\rho_0 = 2.65$  g/cm<sup>3</sup>), quartzite ( $\rho_0 = 2.65$  g/cm<sup>3</sup>) and novaculite ( $\rho_0 = 2.64$  g/cm<sup>3</sup>) shown in Figure 5, support the above interpretation of the combination of pressure-density and shock temperatures. Here  $V_p$  is the longitudinal (non-zero rigidity) elastic velocity of the solid, whereas  $V_B$  is the bulk plastic velocity of the deformed solid and above ~107 GPa, the velocity of shock-induced melt. The rarefaction velocities for elastic and deformational unloading demonstrate that the stishovite compressional wave velocity increases to about 12.9 km/s, at 35 GPa. At this pressure mode softening (decreasing shear modulus), begins to occur [Cohen, 1991]. With increasing pressure the sound velocity decreases in anticipation of

**Table 2.** Transition Energies<sup>a</sup>

Phase 1	Phase 2	Transition Energy (MJ/kg)
Cristobalite	$\alpha$ -quartz	0.056 <sup>b</sup>
Fused quartz	$\alpha$ -quartz	0.70 <sup>c</sup>
$\alpha$ -quartz	Stishovite	0.86 <sup>b</sup>
Coesite	Stishovite	0.82 <sup>b</sup>
Stishovite	CaCl <sub>2</sub>	0.5
$\alpha$ -quartz	melt	2.5

<sup>a</sup> $\Delta E \cong \Delta H$  at ambient conditions.<sup>b</sup>Navrotsky [1995].<sup>c</sup>Richet and Bottinga [1986].

**Figure 5.** Sound speed measurements in SiO<sub>2</sub> phases with  $\rho_0 = 2.65$  g/cm<sup>3</sup>.  $V_p$  versus pressure curve was calculated by *Carpenter et al.* [2000]. Quartz data of *McQueen* [1992] below 90 GPa not plotted.



the  $\sim 65$  GPa transition to the  $\text{CaCl}_2$  structure. The compressional wave velocity in the  $\text{CaCl}_2$  structure (metastably shocked into the melt region above 80 GPa) then rises again until at 115 GPa catastrophic melting occurs. At this pressure the longitudinal velocity becomes equal to the bulk velocity, as is expected upon melting.

[16] In contrast, the bulk sound velocity steadily increases at the onset of the stishovite to  $\text{CaCl}_2$  structure transition and continues to increase with pressure. Quite interestingly the bulk sound velocities data appear to change little upon catastrophic melting of  $\text{CaCl}_2$  structure at  $\sim 115$  GPa. This implies the bulk modulus of solid  $\text{SiO}_2$  in the  $\text{CaCl}_2$  structure is essentially equal to that of the melt. If other silicates behave similarly, then in contrast to the conclusion of Karato and Karki [2001] the presence of a small fraction of melt in the lowermost mantle may remain a viable explanation for the high values of  $(\partial \ln V_s / \partial \ln V_p)$  as discussed by Duffy and Ahrens [1992].

## 6. Conclusions

[17] The shock wave pressure-density data for cristobalite and porous coesite are consistent with these phases transforming from their initial state to the stishovite structure upon shock compression. Above 40–50 GPa, transformation to stishovite is complete and shock-induced transformation to the melt begins at 65 GPa in cristobalite, and  $\sim 85$  GPa in porous coesite. Based on shock temperature measurements in fused and crystal silica, we infer that in cristobalite, fused silica and porous coesite the solid is superheated in the stishovite structure starting at 45, 55 and 60 GPa, respectively. In contrast, shock induced transformation to stishovite from initially crystal quartz and coesite begins at 22 and 30 GPa, respectively. Complete transformation to stishovite is completed at 40–50 GPa along their Hugoniot and transformation to the  $\text{CaCl}_2$  structure begins at 65–75 GPa. The  $\text{CaCl}_2$  phase for crystal quartz and coesite is metastably superheated above the 80 GPa, 4000 K melting line of the  $\text{CaCl}_2$  structure. Catastrophic melting occurs at  $\sim 115$  GPa along the quartz Hugoniot, and is expected to occur at  $\sim 137$  GPa along the coesite Hugoniot shocked into the  $\text{CaCl}_2$  structure. At higher pressures the Hugoniot of crystal quartz and coesite lie in the melt regime.

[18] **Acknowledgments.** Research supported by NSF. JAA appreciates the support of Sandia National Laboratory where a substantial portion of this study was performed. We appreciate receiving preprints from Wendy Panero. Helpful reviews by Denis Andrault, Sarah Stewart-Mukhopadhyay, Ahmed El Goresy, and Paul Asimow are appreciated. Contribution number 8859, Division of Geological and Planetary Sciences, California Institute of Technology.

## References

- Adadurov, G. A., et al., Shock compression of quartz, *Prikl. Mekh. Fiz.*, 81–89, 1962.
- Ahrens, T. J., G. A. Lyzenga, and A. C. Mitchell, Temperatures induced by shock waves in minerals, in *High Pressure Research in Geophysics*, vol. 12, edited by S. Akimoto and M. H. Manghnani, pp. 579–594, Center for Academic Publications, Japan, 1982.
- Andrault, D., et al., Pressure-induced Landau-type transition in stishovite, *Science*, 282, 720–724, 1998.
- Borshchevskii, A. O., M. M. Gorshkov, and A. M. Tarasov, The two-stage shock compression of quartzite to pressures of 550–1500 kbar, *Izv. Earth Phys.*, 34, 291–294, 1998.
- Boslough, M., Postshock temperatures in silica, *J. Geophys. Res.*, 93, 6477–6484, 1988.
- Carpenter, M. A., R. J. Hemley, and H. K. Mao, High-pressure elasticity of stishovite and the  $\text{P4}_2/\text{mm}$  to  $\text{Pnmm}$  phase transition, *J. Geophys. Res.*, 105, 10,807–10,816, 2000.
- Chao, E. C. T., et al., Stishovite,  $\text{SiO}_2$ , a very high pressure new mineral from Meteor Crater, Arizona, *J. Geophys.*, 67, 419–421, 1962.
- Cohen, R. E., Bonding and elasticity of stishovite  $\text{SiO}_2$  at high pressure-linear augmented plane wave calculations, *Am. Mineralogist*, 76, 733–742, 1991.
- DeCarli, P. S., and D. J. Milton, Stishovite: Synthesis by shock wave, *Science*, 147, 144–145, 1965.
- Dubrovinskaya, N. A., et al., Direct transition from cristobalite to post-stishovite  $\alpha\text{-PbO}_2$ -like silica phase, *Euro. J. Mineral.*, 13, 479–483, 2001.
- Dubrovinsky, L. S., et al., Experimental and theoretical identification of a new high-pressure phase of silica, *Nature*, 388, 362–365, 1997.
- Dubrovinsky, L. S., et al., Pressure-induced transformations of cristobalite, *Chem. Phys. Lett.*, 333, 264–270, 2001.
- Duffy, T. S., and T. J. Ahrens, Lateral variations in lower mantle seismic velocity, in *High-Pressure Research: Application to Earth and Planetary Sciences (Geophysical Monograph 67)*, vol. 3, edited by Y. Syono and M. H. Manghnani, pp. 197–205, Terra Scientific, Tokyo, Japan, 1992.
- El Goresy, A., et al., A monoclinic post-stishovite polymorph of silica in the Shergotty Meteorite, *Science*, 288, 1632–1634, 2000.
- Fowles, R., Dynamic compression of quartz, *J. Geophys. Res.*, 72, 5729–5742, 1967.
- Karato, S., and B. B. Karki, Origin of lateral variation of seismic wave velocities and density in deep mantle, *J. Geophys. Res.*, 106, 21,771–21,783, 2001.
- Kingma, K. J., et al., Transformation of stishovite to a denser phase at lower-mantle pressures, *Nature*, 374, 243–245, 1995.
- Lu, K., and Y. Li, Homogeneous nucleation catastrophe as a kinetic stability limit for superheated crystal, *Phys. Rev. Lett.*, 80, 4474–4477, 1998.
- Luo, S.-N., et al., Stishovite and its implications in geophysics: New results from shock-wave experiments and theoretical modeling, *Uspekhi Physics Nauk.*, in press, 2002.
- Lyzenga, G. A., T. J. Ahrens, and A. C. Mitchell, Shock temperatures of  $\text{SiO}_2$  and their geophysical implications, *J. Geophys. Res.*, 88, 2431–2444, 1983.
- Marsh, S. P., (Ed.), *LASL Shock Hugoniot Data*, pp. 1–658, University of California Press, Berkeley, 1980.
- McQueen, R. G., The velocity of sound behind strong shocks in  $\text{SiO}_2$ , in *Shock Compression of Condensed Matter 1991*, edited by S. C. Schmidt, R. D. Dick, J. W. Forbes, and D. G. Tasker, pp. 75–78, Elsevier, 1992.
- McQueen, R. G., and J. N. Fritz, Some techniques and results from high-pressure shock-wave experiments utilizing the radiation from shocked transparent materials, in *Shock Wave in Condensed Matter - 1981*, edited by W. J. Nellis, L. Seaman, and R. A. Graham, pp. 193–207, Am. Inst. Phys., New York, 1982.
- McQueen, R. G., J. N. Fritz, and S. P. Marsh, On the equation of state of stishovite, *J. Geophys. Res.*, 68, 2319–2322, 1963.
- Navrotsky, A., Thermodynamic properties of minerals, in *Mineral Physics & Crystallography: A Handbook of Physical Constants*, edited by T. J. Ahrens, pp. 18–28, American Geophysical Union, Washington DC, 1995.
- Panero, W. R., and R. Jeanloz, Equation of state of stishovite, *Abstract, EOS Trans. Amer. Geophys. U.*, 81, 535, 2000.
- Podurets, M. A., G. V. Simakov, and R. F. Trunin, On the phase equilibrium in shock-compressed quartz and the kinetics of phase transitions, *Physics of the Solid Earth*, 12, 419–424, 1976.
- Podurets, M. A., G. V. Simakov, and R. F. Trunin, Stishovite transition to a denser phase, *Izvestiya, Earth Physics*, 26, 295–300, 1990.
- Richet, P., and Y. Bottinga, Thermochemical properties of silicate glasses and liquids: A review, *Rev. Geophys.*, 24, 1–25, 1986.
- Stishov, S. M., and S. V. Popova, New dense polymorphic modification of silica, *Geokhimiya*, 10, 839–937, 1961.
- Stixrude, L., and M. S. T. Bukowski, Thermodynamic analysis of the system  $\text{MgO-FeO-SiO}_2$  at high pressure and the structure of the lowermost mantle, in *Evolution of the Earth and Planets, Geophysical Monograph*, vol. 74, pp. 131–141, IUGG, 1993.
- Teter, D. M., et al., High pressure polymorphism in silica, *Phys. Rev. Lett.*, 80, 2145–2148, 1998.
- Trunin, R. F., et al., Dynamic compressibility of quartz and quartzite at high pressure, *Izv. Physics of the Solid Earth*, 1, 8–12, 1971.
- Tsushida, Y., and T. Yagi, A new post-stishovite high-pressure polymorph and silica, *Nature*, 340, 217–220, 1989.
- Wackerle, J., Shock-wave compression of quartz, *J. Appl. Phys.*, 33, 922–937, 1962.
- Weidner, D. J., et al., The single-crystal elastic moduli of stishovite, *J. Geophys. Res.*, 87, 4740–4746, 1982.
- Zhugin, Y. N., et al., Phase transformations in quartz, induced by shock waves from underground nuclear explosions, *Izv. Phys. Solid Earth, transl. Fiz. Zemli*, 35, 478–483, 1999.

J. A. Akins and T. J. Ahrens, Lindhurst Laboratory of Experimental Geophysics, Seismological Laboratory 252-21, California Institute of Technology, Pasadena, CA 91125, USA. (tja@caltech.edu)